AGU PUBLICATIONS

Geophysical Research Letters

RESEARCH LETTER
10.1002/2015GL063239

Key Points:
- Spurious oscillation in insolation is found in CMIP5 model results
- The oscillation is attributed to sampling error in the solar zenith angle
- The spurious oscillation affects regional climate

Supporting Information:
- Readme
- Figure S1
- Figure S2

Correspondence to:
M. Zhang,
Minghua.zhang@stonybrook.edu

Citation:
Zhou, L., M. Zhang, Q. Bao, and Y. Liu (2015), On the incident solar radiation in CMIP5 models, *Geophys. Res. Lett.*, *42*, 1930–1935, doi:10.1002/2015GL063239.

Received 23 JAN 2015
Accepted 3 MAR 2015
Accepted article online 5 MAR 2015
Published online 27 MAR 2015

On the incident solar radiation in CMIP5 models

Linjiong Zhou[1,2,3], Minghua Zhang[3,4], Qing Bao[1], and Yimin Liu[1]

[1]State Key Laboratory of Numerical Modeling for Atmospheric Sciences and Geophysical Fluid Dynamics, Institute of Atmospheric Physics, Chinese Academy of Sciences, Beijing, China, [2]University of Chinese Academy of Sciences, Beijing, China, [3]School of Marine and Atmospheric Sciences, Institute for Terrestrial and Planetary Atmospheres, Stony Brook University, Stony Brook, New York, USA, [4]International Center for Climate and Environment Sciences, Institute of Atmospheric Physics, Chinese Academy of Sciences, Beijing, China

Abstract Annual incident solar radiation at the top of atmosphere should be independent of longitudes. However, in many Coupled Model Intercomparison Project phase 5 (CMIP5) models, we find that the incident radiation exhibited zonal oscillations, with up to 30 W/m^2 of spurious variations. This feature can affect the interpretation of regional climate and diurnal variation of CMIP5 results. This oscillation is also found in the Community Earth System Model. We show that this feature is caused by temporal sampling errors in the calculation of the solar zenith angle. The sampling error can cause zonal oscillations of surface clear-sky net shortwave radiation of about 3 W/m^2 when an hourly radiation time step is used and 24 W/m^2 when a 3 h radiation time step is used.

1. Introduction

The incident solar radiation at the top of atmosphere (TOA) is the most important forcing of the climate system of the Earth. Because of the uncertainty in the measurements of solar constant, climate models may use slightly different values of this constant [*Trenberth et al*., 2009; *Stephens et al*., 2012; *Wild et al*., 2012; *Neale et al*., 2013], but they all employ the same well-known algorithm [*Green*, 1985] to calculate the solar zenith angle that determines the temporal and spatial distributions of insolation. Theoretically, when averaged over a day, insolation is expected to be zonally uniform if the change of solar declination angle within a day is neglected. However, we found that this is not the case in many climate models that participated in the Coupled Model Intercomparison Project phase 5 (CMIP5).

The purpose of this short paper is to report this bias to inform users of CMIP5 results when interpreting the regional and diurnal variations of model results and to call for the attention of the relevant modeling groups to correct this bias in future simulations. We show that this unrealistic model behavior is caused by sampling errors in the radiation calculations, which are accounted for in some models but not in others. The impact of the bias on the simulation of atmospheric radiation and clouds is also presented.

2. Data and Models

The insolation data in different CMIP5 models (see Table S1 in the supporting information for the model names) were downloaded directly from the Earth System Grid. Because insolation is independent of a model's internal climate simulations, we only obtained the monthly mean fields from one ensemble member of each model's Atmospheric Model Intercomparison Project (AMIP) simulation for an arbitrarily selected year. Even though we did not examine results in CMIP3 and earlier phases of the coupled model intercomparison projects, we expect that the CMIP5 model insolation errors also existed in their predecessor models.

To study the cause and correction method of the insolation error, we used the Community Earth System Model (CESM, version1.2.2) (available online at http://www2.cesm.ucar.edu) [*Gent et al*., 2011], which also exhibited the errors. Four year integrations of the CESM are used to assess the impact of the insolation error on the simulated climate. The last 3 years are used for analysis.

3. Results

Annual mean incident solar radiation at TOA from eight selected CMIP5 models is shown in Figure 1. In the figure, we amplified the color scale to highlight the spatial differences in the tropics. It is seen that the

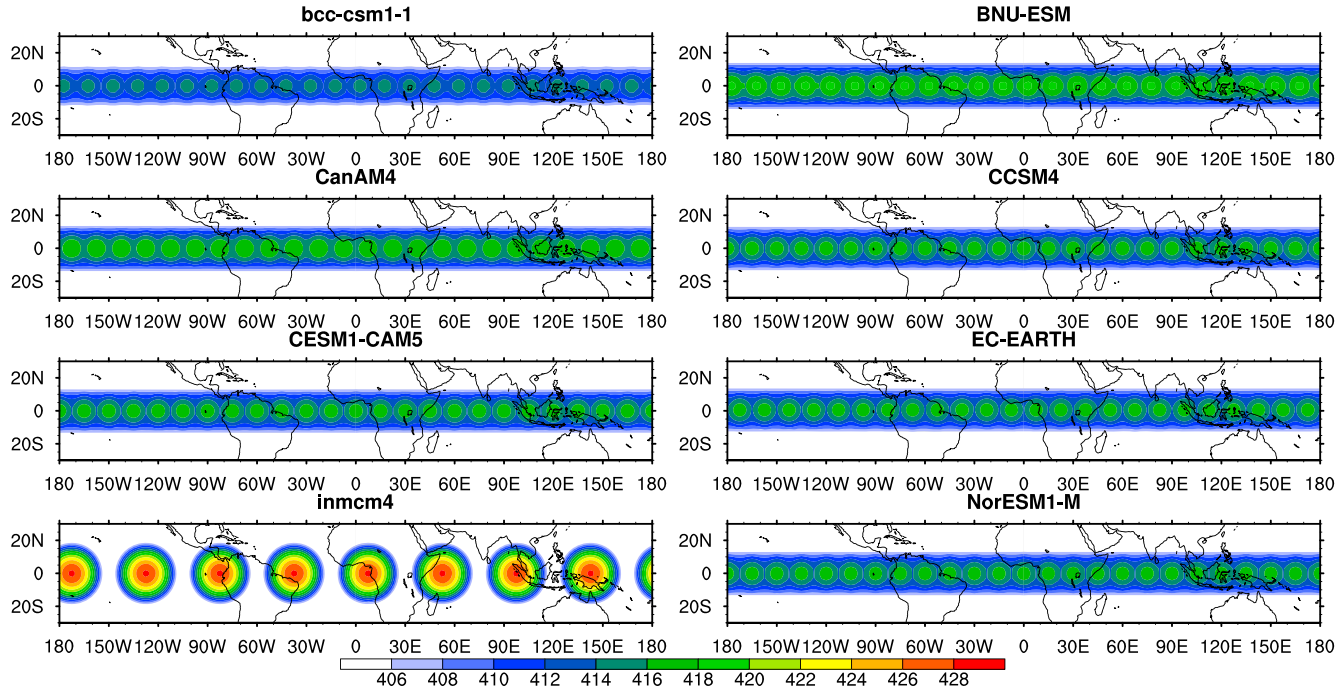

Figure 1. Annual mean incident solar radiation at the top of atmosphere from eight climate models in CMIP5. The color scale has been adjusted to highlight the zonal variation in the tropics. The model names are in Table S1 in the supporting information. Units: W/m^2.

distributions of radiative flux in many models (bcc-csm1-1, BNU-ESM, CanAM4, CCSM4, CESM1-CAM5, EC-EARTH, inmcm4, and NorESM1-M) exhibit longitudinal oscillations. The same type of biases was also reported in some climate model in AMIP-2 in the dezonalized anomalies plot [*Raschke et al.*, 2005]. This variation would not be visible in zonally averaged plots or in spatial plots when the color scale has a large range. Other CMIP5 models are found to exhibit little or no zonal oscillations (ACCESS1-0, ACCESS1-3, CMCC-CM, CNRM-CM5, CSIRO-Mk3-6-0, FGOALS-g2, FGOALS-s2, GFDL-CM3, GFDL-HIRAM-C180, GISS-E2-R, HadGEM2-A, IPSL-CM5A-LR, IPSL-CM5A-MR, IPSL-CM5B-LR, MIROC5, MPI-ESM-LR, MPI-ESM-MR, MRI-AGCM3-2H, MRI-AGCM3-2S, and MRI-CGCM3, see Figure S1 in the supporting information).

CESM is among the models that contain the bias. The spurious feature is found to be the result of approximations introduced in the time discretization of the solar zenith angle. The formula is

$$\cos z_n = \sin\delta \sin\phi + \cos\delta \cos\phi \cos H(t_n), \tag{1}$$

where z is solar zenith angle, ϕ is the latitude, δ is the declination of the Sun, $H \in [-\pi, \pi)$ hour angle of the sun. and $\cos z$ is set to zero when it is negative. In the CESM, the solar zenith angle at each location is calculated at instantaneous time t_n and its value persists until the next radiation time step. For a given day at given latitude, the number of radiation time steps in each day determines the pattern number of zonally distributed insolation field, since each radiation time step has its specific zonal distribution of TOA insolation. CESM used 1 h radiation time step. This corresponds to 24 zonal distributions. To illustrate the impact of the sampling bias, in Figure 2a we used the solar zenith angle at the equator as an example and a 3 h radiation time step to show the eight zonal patterns. When these patterns are summed together, they form a zonally varying distribution with a wave number the same as the pattern number of the instantaneous insolation.

While the above analysis is only for CESM, it is obvious from Figure 1 that this same error exists in many other models. Some models used hourly radiation time steps; one model used a 3-hourly radiation time step. The magnitude of the sensitivity to the radiation time step is shown in Figure 2b for insolation at the equator with a solar constant of 1360 W/m^2. The wave numbers 24, 12, and 8, corresponding to a 1 h, 2 h, and 3 h

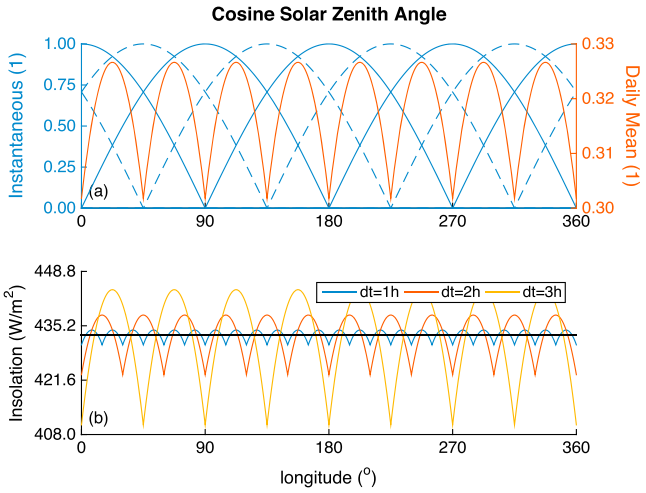

Figure 2. Equatorial (a) instantaneous (blue solid and dashed lines, with the dashed lines used for clarity of the figure) and daily mean (red line) cosine solar zenith angle for 3 h radiation time step based on original algorithm and (b) insolation for 1 h, 2 h, and 3 h radiation time step based on the original algorithm (blue, red, and yellow lines) and the revised algorithm (black horizontal line).

radiation time step, respectively, exhibit differences between the maximum and minimum solar radiation of 3.7 W/m^2, 14.9 W/m^2, 33.8 W/m^2, respectively.

This sampling bias can be removed by taking the average of the cosine solar zenith angle between the two time steps:

$$\begin{aligned}\overline{\cos z_n} &= \frac{1}{\Delta t}\int_{t_n}^{t_n+\Delta t}\cos z(t)\,dt \\ &= \frac{H_+^* - H_-^*}{H_+ - H_-}\sin\delta\sin\phi \\ &\quad + \frac{\sin H_+^* - \sin H_-^*}{H_+ - H_-}\cos\delta\cos\phi\end{aligned} \tag{2}$$

where $H_- \in [-\pi, \pi)$ and $H_+ \in [-\pi, \pi)$ are hour angles at t_n and $t_n + \Delta t$ at each location and $H_-^* = \max[-h, \min(H_-, h)]$, $H_+^* = \max[-h, \min(H_+, h)]$. The hour angle at sunset is h. $\overline{\cos z_n}$ is set to zero when it is negative. Similar time-averaged algorithms have been used in other models [*Russell et al.*, 1995]. We note that in the above equation, the averaging is between time t_n to $t_n + \Delta t$, not centered at t_n. This is consistent with the integration of the thermodynamic equation from t_n *to* $t_n + \Delta t$ to calculate the radiative heating during this time interval. The time averaging eliminates both spatial sampling errors and temporal biases; it conserves the total energy of the insolation. The modification of the code is minimal. The black straight line in Figure 2b is the calculated daily insolation as a function of longitude by using the above revised algorithm with 1, 2, and 3 hourly radiation time steps. The diurnally averaged radiation is independent of longitude and radiation time step as expected from the revised algorithm.

We next assess the impact of the sampling bias of insolation on simulated climate by using the CESM. We included simulations with both 3-hourly and 1-hourly radiation time steps. The simulations with 3-hourly and hourly time steps using the original insolation calculation are referred as exp1 and exp2, while the corresponding simulations using the revised algorithm are referred to as exp3 and exp4. The four AMIP-type experiments are listed in Table 1. Because sea surface temperature (SST) is specified, we do not expect large impact of the revised algorithm on the surface temperature. We therefore show the impact of the revised algorithm on the radiative fluxes and clouds.

Figure 3 (left column) gives the annually averaged radiation fields when the revised algorithm and a 1 h radiation time step are used. From the top to the bottom rows are the downward shortwave radiation at the TOA (SDT), clear-sky net shortwave radiation at TOA (SNTC), total-sky net shortwave radiation at TOA (SNT), clear-sky net shortwave radiation at surface (SNSC), and total-sky net shortwave radiation at surface (SNS). The color scales have been adjusted to highlight the fields in the tropics, which placed some regions with large cloud radiative effects out of the range. As expected, no zonal variation is seen in the insolation field. Since there is hardly any difference between different radiation time steps when the revised algorithm is used, results with 3-hourly radiation time step are not shown here.

Table 1. List of Experiments

Experiment Name	Algorithm	Radiation Time Step	Integration
exp1	Original Algorithm	3 h	AMIP 4 years
exp2	Original Algorithm	1 h	AMIP 4 years
exp3	Revised Algorithm	3 h	AMIP 4 years
exp4	Revised Algorithm	1 h	AMIP 4 years

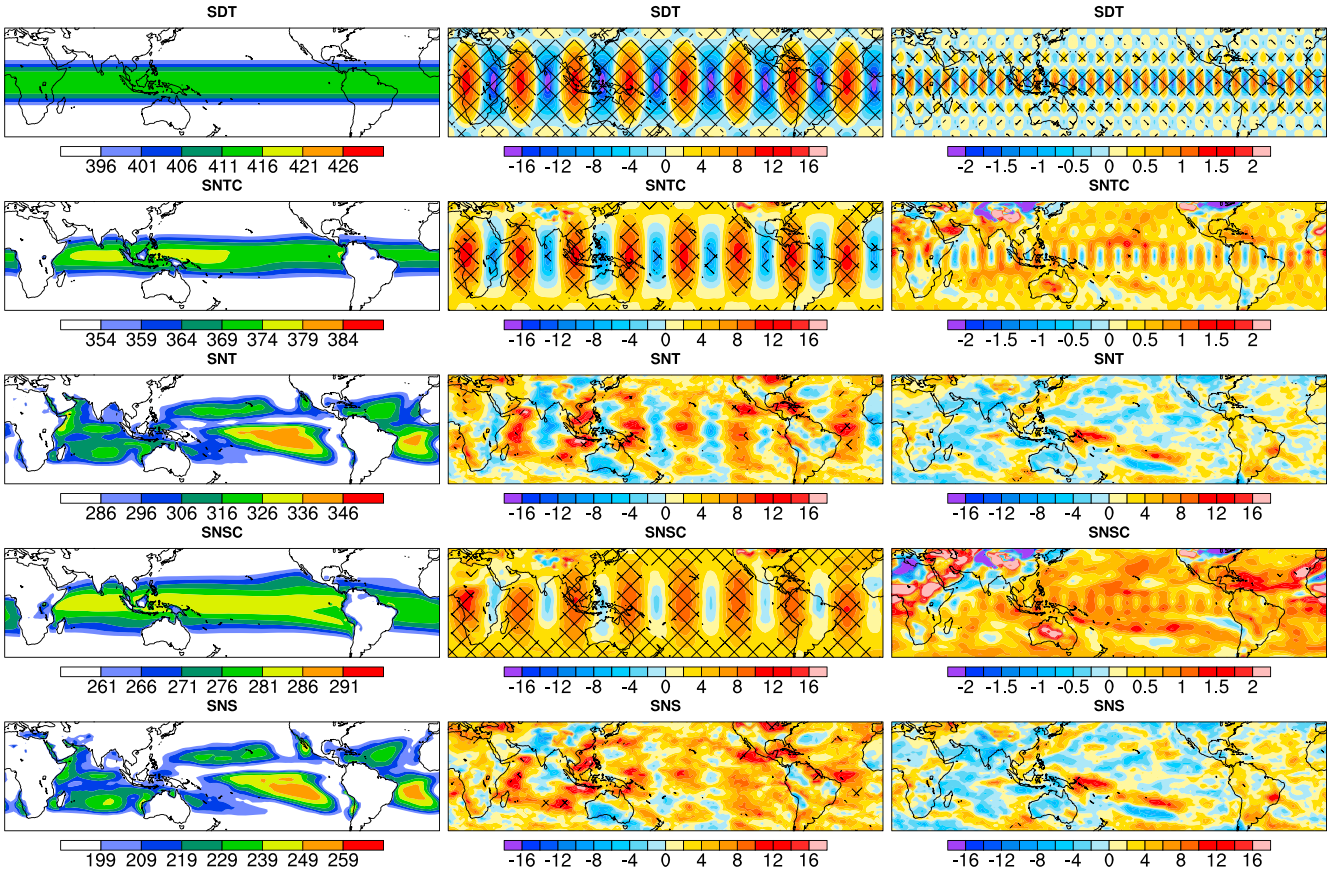

Figure 3. Annual mean downward shortwave radiation at TOA (SDT), clear-sky net shortwave radiation at TOA (SNTC), total-sky net shortwave radiation at TOA (SNT), clear-sky net shortwave radiation at surface (SNSC), total-sky net shortwave radiation at surface (SNS) for (left column) 1 h radiation time step based on the revised algorithm, (middle column) the original algorithm minus the revised algorithm for 3 h radiation time step, (right column) the original algorithm minus the revised algorithm for 1 h radiation time step. Hatched area indicates statistically significant regions at the 95% confidence level. Units: W/m^2.

Figure 3 (middle column) gives the difference of the fields between the original algorithm and the revised algorithm when the radiation time step is 3 h. The difference in the insolation (SDT) has distinctive zonal oscillations in the clear-sky net radiation at both the TOA and surface. For the total-sky fluxes, longitudinal oscillation is also clearly identifiable that is synchronized with that of insolation, but it has been modified by clouds. The oscillation of the total-sky TOA net solar radiation can reach 24 W/m^2 (-12 W/m^2 to 12 W/m^2) in the tropics. Differences between the two algorithms for hourly radiation time step are shown in Figure 3 (right column). The difference patterns are the same as in Figure 3 (middle column) except with smaller scales and much smaller amplitudes. The oscillation of the total-sky TOA net solar radiation reaches about 3 W/m^2 (-1.5 W/m^2 to 1.5 W/m^2) in the tropics.

Figure 4 shows the impact of the insolation sampling bias on cloud-related fields when the 3-hourly radiation time step is used. Figure 4a gives the difference in cloud amount while Figure 4b shows the cloud radiative effect (CRE). Except for the low cloud amount, all fields in Figure 4 are positively correlated with SDT at a statistical significance level higher than 95% (see Table S2 in the supporting information). The amount of high, middle, and total clouds are all impacted by SDT as indicated by the longitudinal oscillations with a range of about 4% (-2% to 2%). At locations where SDT is larger, cloud amount tends to be larger. This is because the atmosphere absorbs more solar radiation when SDT is larger, causing more upward motion that produces more clouds (Figure 4c). SDT has little impact on low clouds, possibly because SST is fixed. Figure 4b also shows the impact on shortwave and longwave radiation cloud effect at TOA is about 8 W/m^2 (-4 W/m^2 to 4 W/m^2) in the shortwave cloud radiative effect and 3 W/m^2 (-1.5 W/m^2 to 1.5 W/m^2) in the longwave cloud radiative effect. As expected, the shortwave and longwave cloud effects are out of phase, but their effects on the atmosphere-Earth system are different—the shortwave effect is primarily on the surface

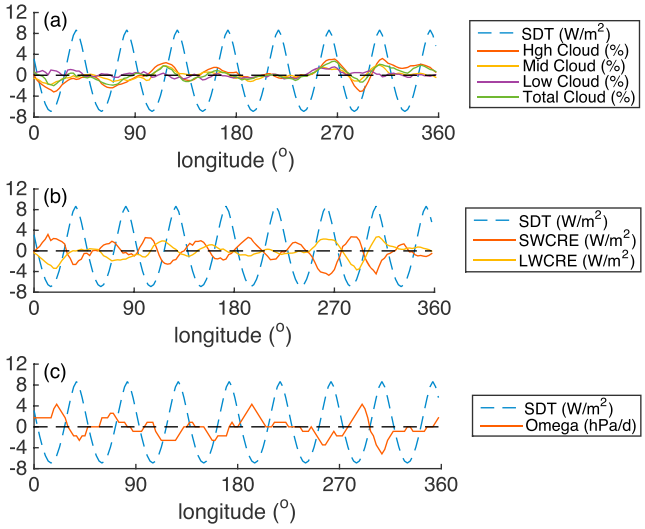

Figure 4. Difference of annual mean downward shortwave radiation at TOA averaged between 40°S to 40°N (SDT, dashed blue line) using 3 h radiation time step, and the corresponding (a) differences in the amount of high, middle, low, and total clouds; (b) differences in TOA shortwave and longwave cloud radiative effect (SWCRE and LWCRE); and (c) difference in the 500 hPa pressure vertical velocity (Omega).

while the longwave effect is primarily in the atmosphere. This impact of the insolation oscillation on the cloud effect is due to the combination of the insolation oscillation itself and its indirect effect on clouds. These two factors compensate each other, with the net impact dominated by the direct impact of the insolation oscillation. The impact of the algorithm on clouds with hourly radiation time step is qualitatively similar but with smaller magnitude. They are 2% in cloud amount and 2 W/m^2 in cloud radiative effect.

Even though these values are small, they represent unphysical features of the model that can be easily avoided in the future. The impacts are in fact nonnegligible because of the stationary impact of the radiation field. With the 3 h radiation time step, the impacts on surface temperature, precipitation, sensible heat, and latent heat fluxes in the tropics are about 0.2 K, 0.5 mm/d, 5 W/m^2, and 5 W/m^2, respectively (see Figure S2 in the supporting information).

4. Summary and Discussion

We have reported an unexpected behavior in the annual mean incident solar radiation at top of atmosphere in many CMIP5 models that displayed spurious zonally varying distributions with amplitude up to 30 W/m^2. We have shown that this bias is caused by temporal sampling errors in the calculation of time mean solar zenith angle in the models.

We applied a revised algorithm in the CESM that corrects the bias from both spatial and temporal sampling errors, guarantees energy conservation, and is easy to implement. In an experimental setting with specified SST, we found that the regionally biased algorithm can cause up to 24 W/m^2 and 3 W/m^2 difference of net surface clear-sky shortwave radiation at the equator when 3-hourly and hourly radiation time steps are used, respectively. Where there is stronger SDT, there is more cloud fraction and larger shortwave radiation cloud effect.

Even though the regional biases in insolation can be averaged out over the globe, they may cause spurious variation of regional climate or diurnal variability. We did not carry out coupled model simulations to assess the climate impact on surface temperature of the different algorithms, but since what we reported is a true deficiency in some climate models, we caution users of CMIP5 results of this deficiency in some models and advocate the use of the correct algorithm in CMIP6 and other future simulations by these models.

Acknowledgments
We would like to thank Haiyang Yu, Shuaiqi Tang, Yuwei Wang, Jianhua Lu for useful discussion of the results. We acknowledge the World Climate Research Programme's Working Group on Coupled Modelling, which is responsible for CMIP, and we thank the climate modeling groups for producing and making available their model output. For CMIP, the U.S. Department of Energy's Program for Climate Model Diagnosis and Intercomparison provided coordinating support and led the development of software infrastructure in partnership with the Global Organization for Earth System Science Portals. This research is supported by the Major National Basic Research Program of China (973 Program) on Global Change under grant 2010CB951800 and by CAS XDA10010402. Additional support was provided by the Biological and Environmental Research Division in the Office of Sciences of the US Department of Energy (DOE) and by National Science Foundation to the Stony Brook University. All data used in this paper are available upon request.

The Editor thanks Jonathan Jiang and two anonymous reviewers for their assistance in evaluating this paper.

References

Gent, P. R., et al. (2011), The Community Climate System Model Version 4, *J. Clim.*, *24*(19), 4973–4991, doi:10.1175/2011jcli4083.1.
Green, R. M. (1985), *Spherical Astronomy*, 533 pp., Cambridge Univ. Press, Cambridge, U. K., and New York.
Neale, R. B., J. Richter, S. Park, P. H. Lauritzen, S. J. Vavrus, P. J. Rasch, and M. Zhang (2013), The mean climate of the Community Atmosphere Model (CAM4) in forced SST and fully coupled experiments, *J. Clim.*, *26*(14), 5150–5168, doi:10.1175/JCLI-D-12-00236.1.
Raschke, E., M. A. Giorgetta, S. Kinne, and M. Wild (2005), How accurate did GCMs compute the insolation at TOA for AMIP-2?, *Geophys. Res. Lett.*, *32*, L23707, doi:10.1029/2005GL024411.
Russell, G. L., J. R. Miller, and D. Rind (1995), A coupled atmosphere-ocean model for transient climate change studies, *Atmos. Ocean*, *33*(4), 683–730, doi:10.1080/07055900.1995.9649550.

Stephens, G. L., J. Li, M. Wild, C. A. Clayson, N. Loeb, S. Kato, T. L'Ecuyer, P. W. Stackhouse, M. Lebsock, and T. Andrews (2012), An update on Earth's energy balance in light of the latest global observations, *Nat. Geosci.*, *5*(10), 691–696, doi:10.1038/ngeo1580. [Available at http://www.nature.com/ngeo/journal/v5/n10/abs/ngeo1580.html.]

Trenberth, K. E., J. T. Fasullo, and J. Kiehl (2009), Earth's global energy budget, *Bull. Am. Meteorol. Soc.*, *90*(3), 311–323, doi:10.1175/2008bams2634.1.

Wild, M., D. Folini, C. Schär, N. Loeb, E. G. Dutton, and G. König-Langlo (2012), The global energy balance from a surface perspective, *Clim. Dyn.*, *40*(11–12), 3107–3134, doi:10.1007/s00382-012-1569-8.